Investigation of tribo-mechanical performance of alkali treated rice-husk and polypropylene-random-copolymer based biocomposites

Fahad Ali Rabbani [a], Muhammad Sulaiman [a], Fatima Tabasum [a], Saima Yasin [b], Tanveer Iqbal [a], Muhammad Shahbaz [a], M.A. Mujtaba [c], Shahid Bashir [d], H. Fayaz [e,*], C Ahamed Saleel [f]

[a] Department of Chemical, Polymer and Composite Materials Engineering, UET Lahore, New Campus, Kala Shah Kaku 39020, Pakistan
[b] Department of Chemical Engineering, UET Lahore, Main Campus, Lahore 54890, Pakistan
[c] Department of Mechanical Engineering, UET Lahore, New Campus, Kala Shah Kaku 39020, Pakistan
[d] Higher Institution Centre of Excellence (HICoE), UM Power Energy Dedicated Advanced Centre (UMPEDAC), Level 4, Wisma R&D, Universiti Malaya, Jalan Pantai Baharu, 59990 Kuala Lumpur, Malaysia
[e] Modeling Evolutionary Algorithms Simulation and Artificial Intelligence, Faculty of Electrical & Electronics Engineering, Ton Duc Thang University, Ho Chi Minh City, Viet Nam
[f] Department of Mechanical Engineering, College of Engineering, King Khalid University, Asir-Abha 61421, Saudi Arabia

ABSTRACT

This study was based on the experimental performance evaluation of a wood polymer composite (WPC) that was synthesized by incorporating untreated and treated rice husk (RH) fibers into a polypropylene random copolymer matrix. The submicron-scale RH fibers were alkali-treated to modify the surface and introduce new functional groups in the WPC. A compatibilizer (maleic anhydride) and a thermos-mechanical properties modifier (polypropylene grafted with 30 % glass fiber) were used in the WPC. The effects of untreated and treated RH on the WPC panels were studied using FESEM, FTIR, and microscope images. A pin-on-disk setup was used to investigate the bulk tribological properties of PPRC and WPC. The complex relationship between the friction coefficient of different loading of RH fibers in the WPC, as a function of sliding distance, was analyzed along with the temperature and morphology of the surface. It was observed that untreated RH acted as a friction modifier, while treated RH acted as a solid lubricant. Microhardness was calculated using the QCSM module on nanoindentation. It was found that untreated RH led to an increase in microhardness, while treated RH caused a decrease in hardness compared to PPRC.

1. Introduction

In our rapidly evolving technological world, advanced materials play a pivotal role in supporting the development of modern industries. Traditional materials such as ceramics, metals, and polymers often fall short in addressing certain specialized needs. This inadequacy has been felt especially in sectors such as aerospace, automotive, and civil engineering, where high performance and durability are paramount. Recognizing this, scientists and engineers have increasingly turned to composite materials [1–3]. These materials, particularly polymer matrix composites, are celebrated for their exceptional strength-to-weight ratios, enabled by the

Fig. 1. Schematic Diagram for Physio-Chemical Pretreatment of Biowaste Rice Husk.

integration of fillers and the variety of manufacturing techniques available [4].

The shift towards sustainable solutions and the urgent need for waste management has propelled the interest in biocomposites [5]. One of the most promising directions in composite material research is the incorporation of natural fillers derived from biowaste, such as banana, bamboo, coconut shell, and notably, rice husk. These materials present a win-win scenario: not only are they efficient reinforcements for polymers, but they also provide an environmentally friendly alternative to synthetic fillers, addressing global environmental concerns [6].

Among these, wood polymer biocomposites (WPC) stand out. These composites, typically constituted of a polymer matrix with wood or biowaste fillers, have seen widespread application due to their enhanced modulus and reduced ductility [5]. Their cost-effectiveness and versatility further boost their appeal for industrial applications [7]. However, the usage of natural fibers is not without challenges. They often present difficulties like moisture susceptibility, variable mechanical properties, and processing issues. Mitigating these challenges involves not only an understanding of the material properties but also optimizing filler-to-matrix ratios, filler size reduction, and the use of compatibilizers [4,8]. Focusing on rice-husk (RH) as a reinforcement filler, it stands out due to its abundance, biodegradability, and high cellulose content. It's been used across various materials, impacting their mechanical, tribological, and thermal properties [6,9–14]. The literature on the tribological behavior of rice husk-based biocomposites, though growing, remains in its infancy [15,16].

Tribology, the study of friction, wear, and lubrication, is pivotal in material selection. It aids in understanding material interactions, guiding the development of efficient mechanical systems and ensuring longevity and reliability [17]. Given this, the current study seeks to delve into the tribological behavior of rice husk-based biocomposites, particularly in a polypropylene random copolymer (PPRC) matrix. Preliminary findings suggest that untreated rice husk often fails to adhere adequately to the PPRC matrix. However, advancements in the field, coupled with the aid of compatibilizers and a variety of pretreatment methods, promise to significantly improve this adhesion [18–20].

To characterize our composites, we employed Fourier-Transform Infrared Spectroscopy (FTIR), Field Emission Scanning Electron Microscopy (FESEM), and microscopic imaging. These analytical tools have proven instrumental in previous studies on similar composites, revealing insights into material behaviors and properties [21]. For the evaluation of the tribological properties, a tribometer was utilized to measure the friction coefficient. Additionally, we incorporated nanoindentation techniques to determine the Vickers Hardness of the biocomposite [22–24]. By integrating these analytical methods, this article seeks to illuminate the potential of rice husk-based biocomposites as substitutes for wood in specific applications, especially where frictional environments are a concern. As the global push towards sustainable and environmentally friendly materials grows, studies like ours pave the way for innovative solutions that cater to both industrial demands and environmental imperatives.

2. Materials and methodology

2.1. Materials

Polypropylene random copolymer (PPRC, trade name R200P, melt index 0.25 g/10 min at 230 °C, with constant load 2.16 kg and density 0.90 g/cm^3), was purchased from Topiline, Seoul, Korea and used with pretreatment. Maleic anhydride (MA, 98 %) was purchased from Unichem, India. Bio waste rice husk (BRH) was collected from a local rice industry Sheikhupura, Pakistan. Polypropylene reinforced with 30 % glass fiber (PPGF, trade name KPG1030, and density 1.14 g/cm^3), was purchased from Kopla Co., Ltd., Hwasoeng, Korea. Sodium hydroxide (NaOH, 99 %) was purchased from Unichem, India. All the reagents and chemicals were of
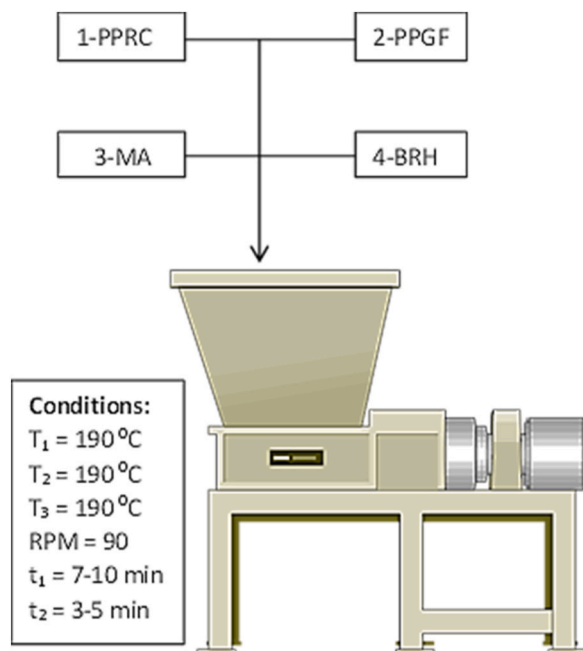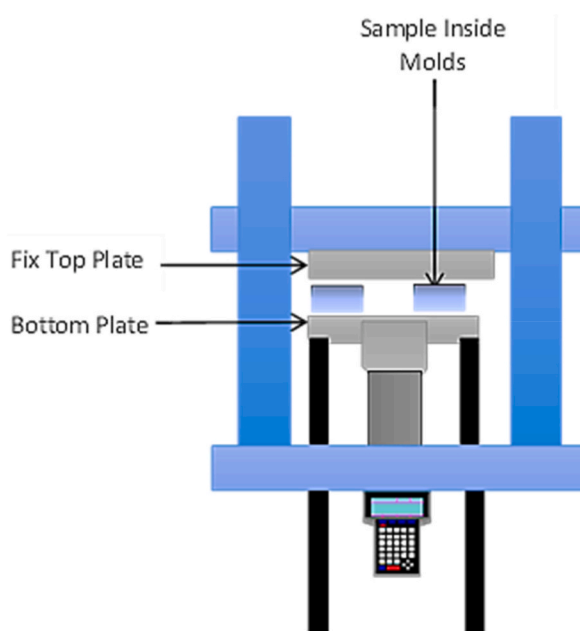
Fig. 2. Melt mixing of Different RawMaterials.

Fig. 3. Thermal HydraulicCompression Molding.

analytical grade.

2.2. Physio-Chemical Pretreatment of Biowaste Rice Husk

Process flow diagram is shown in Fig. 1. Briefly, rice husk was washed with distilled water to remove dust and other contaminants. Then dried at 70 °C in an oven for 24 h, milled and sieved under 48-mesh US Tayler sieve to get particles with diameter of less than 295 μm [25]. The sample was stored in a plastic zipper bag for further processing.

For chemical pretreatment of rice husk, a 10 %w/v of milled rice husk (RH) was soaked in 1-M solution of NaOH and placed in a hot

Table 1
Composition of WPC samples.

Samples Name	PPRC (%)	RH (%)	RHT (%)	MA (%)	PPGF (%)
PPRC	100	–	–	–	–
20RH	76	20	–	2	2
27RH	68.5	27.5	–	2	2
35RH	61	35	–	2	2
42RH	53.5	42.5	–	2	2
50RH	46	50	–	2	2
20RHT	76	–	20	2	2
27RHT	68.5	–	27.5	2	2
35RHT	61	–	35	2	2
42RHT	53.5	–	42.5	2	2
50RHT	46	–	50	2	2

bath shaker operating at 80 °C for 4h, under mild oscillations. After 4 h, the mixture was filtered, washed with distilled water until a neutral pH was achieved and dried in a tray drier at 80 °C for 4 h. The alkali treated rice husk (RHT) samples were collected and stored in zipper bag for further use.

2.3. Fabrication of wood polymer composite *b*oards

Initially, PPRC granules were added to a pre-heated twin-screw batch mixer (Banbury internal mixer, model SBI-35L, Well Shyang Machinery Co., Ltd., Taiwan) as shown in Fig. 2. The mixer consisted of a heating chamber with three zones of temperature controller and two helical mixers rotating in reverse direction. The heating chamber was preheated to 180–190 °C and axial mixer speed was set to 90 rpm. PPGF was added to internal mixer after obtaining homogeneous melt of PPGF following MA was added gradually and heated for 7–10 min (t1). Finally, RH (treated or untreated) was added and mixed for 3–5 min (t2).d

After complete mixing, the semi-solid wood polymer composite (WPC) was removed and inserted into molds. These molds compressed in a hydraulic thermal press (hydraulic platen press, Hartek Technologies Ltd., Gaungzhou, China) operating at 190 °C and 2000 kPa for 10 min, as shown in Fig. 3. Next, the heaters of hydraulic thermal press were turned off and samples were cooled down under compression condition until room temperature reached. The samples were removed from molds and stored for further characterization. Table 1 indicates the compositions of PPRC, PPGF, MA and RH (treated or untreated) determined by Design Expert software using mixture matrix [25].

3. Characterizations

3.1. FTIR analysis

FTIR analysis on different samples was performed using JASCO FT/IR 4600 (Japan). The wavelength of spectrometer was set to 500-4000 cm^{-1} with scan resolution of 4 cm^{-1}. The wavenumber input variable was observed as influencing the transmitted mode of radiation.

3.2. Morphological study (FESEM)

A field emission scanning electron microscope, Helious Nanolab G3 UC (FEI company, USA) was used to analyze surface morphology of selected samples. Since the samples were not conductive, platinum coating was applied using an AGAR High Resolution Coater (AGB7234, UK) before they were loaded into the FESEM.

3.3. Coefficient of Friction (CoF)

To examine CoF and wear characteristics, the synthesized biocomposite samples were loaded on Pin-on-Disk type Tribometer (Microtest, Germany) and analyzed under ASTM G-99.

A flat sample was loaded onto a circular stage disc and secured with screws to prevent any movement of the sample from interfering with the testing. After that, a weight of 10 N was added to the weight pin that had previously made contact with the surface sample. The holding pin for the weight is a cylindrical rod with a 4 mm stainless steel ball at its end. The integrated computer monitored the surface stress in relation to the force used to rotate the circular stage at a preset sliding distance (500 m) and revolution per minute (200 rpm) [26]. The coefficient of friction can therefore be determined by using Equation (1) [27]:

$$\mu = (\text{Frictional measured force}) \, / \, (\text{Applied force}) \tag{1}$$

Where μ is coefficient of friction. Temperature increment of surface due to friction was continuously measured by K-type wire thermocouple integrated with computer software.
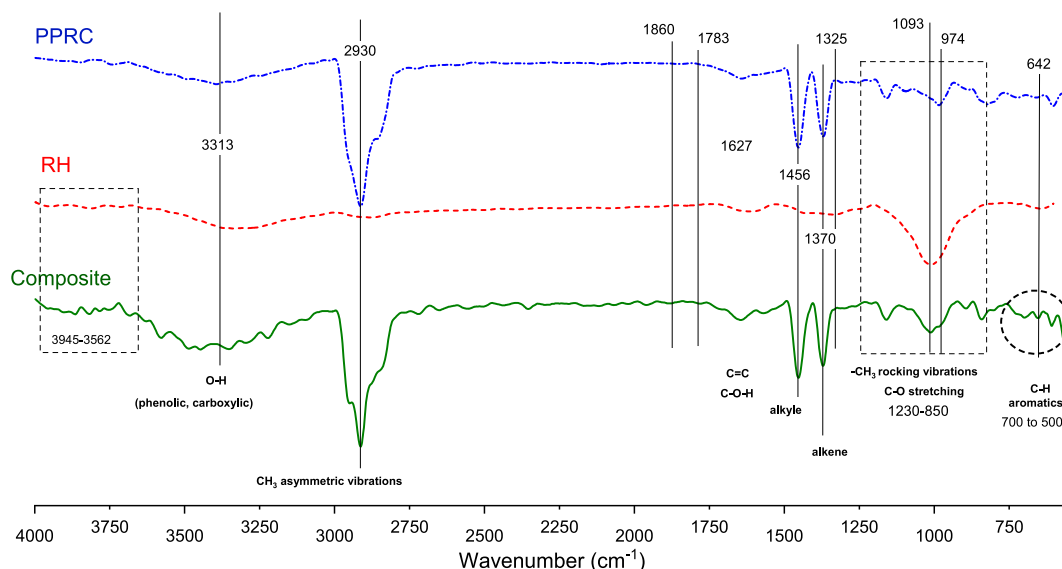
Fig. 4. FTIR analysis of neat PPRC, RH, and Composite.

3.4. Wear measurement

Wear loss is a property of materials which describes loss in weight. Therefore, before and after each test, WPC panels were weighed (±0.001g) to calculate wear loss due to tribological effect. Wear percentage was calculated using Equation (2) [28]:

$$Wear\% = (initial\ weight\ \text{-}\ final\ weight)\ /(initial\ weight) \times 100 \qquad (2)$$

3.5. Vickers Microhardness

The Vickers microhardness test was performed on biocomposites samples using the nano-indentation (KG-ULM from Zwick GmbH & Co. KG, Ulm, Germany). A diamond pyramid indenter was used to indent into surface of the sample at a controlled rate of 18 μm/s. Hardness values were determined by subjecting samples to the indenter under a 100 mN normal load for a designated duration of time.

Hardness is defined ratio of test force F and contact area A. For different samples test, nanoindentation Vickers microhardness (HV) was calculated by Equation (3):

$$HV = Fmax\ /\ A \qquad (3)$$

Where Fmax is the stress at the maximum possible penetration during an indentation cycle, and A is the contact area under the applied load which is $A = 25.5hc^2$. Where hc is contact depth. Hardness value is recorded by the integrated software attached to the nano indenter.

4. Results and discussion

4.1. FTIR analysis

Fig. 4 illustrates the FTIR spectra of neat PPRC, RRH, and their composite. FTIR analysis was conducted to ascertain the unique characteristics imparted to the biocomposite by incorporating RH into PPRC. The Fourier transform infrared spectrometer (FTIR) provides insight into the grafting process between rice husk (RH) and polypropylene random copolymer (PPRC). This is achieved by identifying new peaks that emerge due to the grafting of maleic anhydride.

The FTIR spectra showcase band vibrations ranging from 3750 to 3950 cm⁻¹ to 3562-250 cm⁻¹, suggestive of the presence of –OH functional groups linked to phenylic and carboxylic bonds in RH and the composite [29]. These peaks primarily originate from the cellulosic component of the RH fiber and play a significant role in influencing the composite's overall spectrum.

Moreover, peaks at 2930 cm⁻¹, 1456 cm⁻¹, 1370 cm⁻¹, and 1167 cm⁻¹ correspond to the fundamental structural vibrations of polypropylene [30]. Specifically, they represent alkene symmetrical stretching, alkyl asymmetrical stretching, alkene linkages in PP fibers, and alkene rocking vibrations. A distinct peak at 1670 cm⁻¹ denotes carboxylic linkages in the rice husk fiber, a trait reflected in the composite spectrum. It's noteworthy that the RH-specific peak at 1093 cm⁻¹, absent in the PPRC spectrum, emerges prominently in the composite, underscoring its incorporation [31]. Concurrently, the shift from PPRC's band at 974 cm⁻¹ to the biocomposite's 1009 cm⁻¹ highlights the pronounced stretching of the -C-O group in the biocomposite [30]. The OH stretching typical of cellulose and water
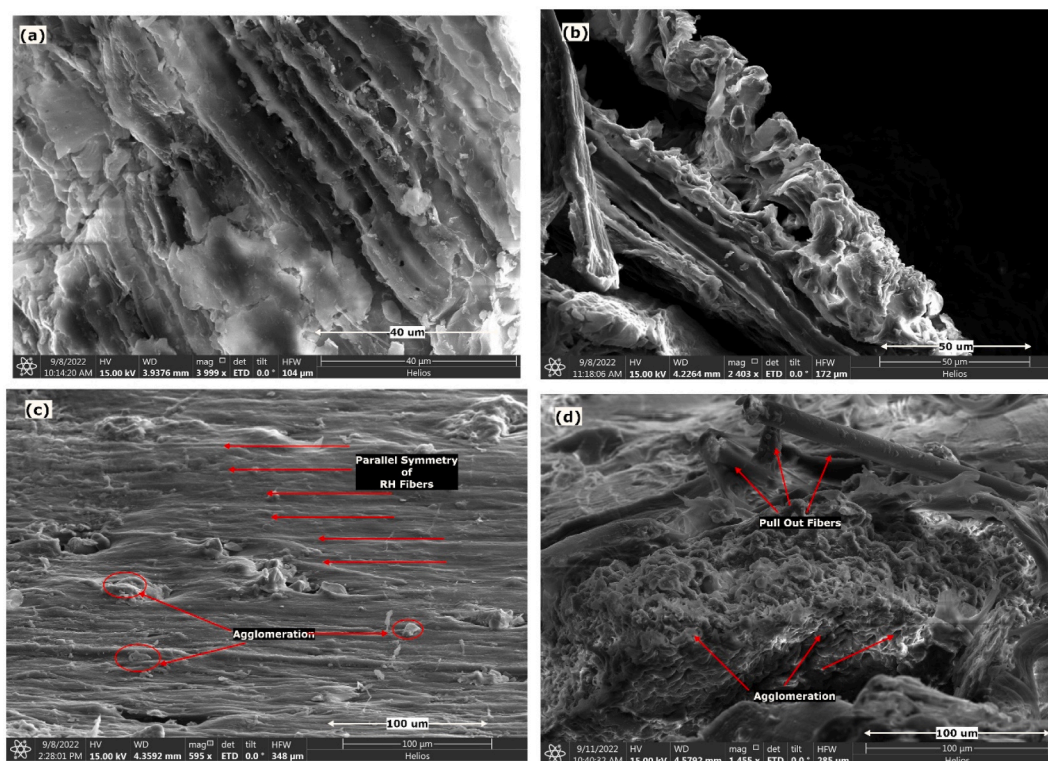
Fig. 5. FESEM of (a) Untreated Rice Husk, (b) Treated Rice Husk, (c) Cross Section of Fractured WPC synthesized from Untreated Rice Husk, and (d) Cross Section of Fractured WPC synthesized from Treated Rice Husk.

molecules in the 3200–3800 cm^{-1} range—originally exclusive to the RH fiber—also materialized in the composite spectrum, suggesting an effective bond between the RH fiber and the PPRC matrix.

Additionally, minor peaks appearing between 700 cm^{-1} and 500 cm^{-1} in the composite spectrum allude to aromatics associated with PPRC's alkyl component. This aromatic signature, especially in the 500–700 cm^{-1} range, acts as a marker for the coupling agent maleic anhydride, thereby reaffirming its grafting and subsequent role in the composite [32].

Upon juxtaposing the spectra of PPRC and the composite, the emergence of new absorption bands is evident. These bands, resonating at 1783 cm^{-1} and 1860 cm^{-1}, correspond to the stretching vibration of carbonyl groups (C═O) in MAH and bolster the premise of successful MAH grafting onto the composite.

4.2. FESEM analysis

Particles with a granulometry of under 295 μm were isolated and subjected to Field Emission Scanning Electron Microscopy (FESEM) analysis. Fig. 5a elucidates the surface topography of the untreated rice husk, while Fig. 5b delineates the morphology of the alkali-treated rice husk. The structural transformation in the morphology due to alkali treatment is evident. In the untreated RH specimen, a discernible presence of cellulosic fibers cemented cohesively with hemicellulose and lignin matrices is observed. This interconnected web-like matrix can be attributed to the lignin component, which consolidates the cellulosic fibers and envelops them, conferring protection to the fiber aggregates [33].

In contrast, the alkali-treated RH specimen manifests a disaggregated fibril structure, appearing in an expanded, lax configuration with diminished fiber length. This morphology induces enhanced porosity and a refined surface topography, with softer tissue regions emerging juxtaposed against compacted and oriented fiber bundles [29].

Moving on to the biocomposites, Fig. 5c and d illustrate the cross-sectional surface area of fractured WPC samples synthesized from untreated rice husk (RH) and alkali-treated rice husk (RHT), respectively. For the untreated RH biocomposite, pull-off fibers at the edges indicate weak adhesion between the fiber and matrix at the surface, although the fiber networks are aligned and homogeneously dispersed, enhancing mechanical properties and surface hardness.

In stark contrast, the biocomposite with alkali-treated rice husk displays a marked morphological alteration. An evident interlocking between matrix and fiber phases leads to a cohesive structure. However, this structure appears heterogenous, potentially due to the truncated fiber length and observed fiber agglomeration in the RHT WPC. Such fiber orientation irregularity might compromise surface hardness and amplify porosity, impacting the material's overall mechanical attributes [34,35]. Notably, in the alkali-treated samples, the RH fibers appear enveloped by the matrix, a characteristic that may mitigate abrasion during tribological interactions,
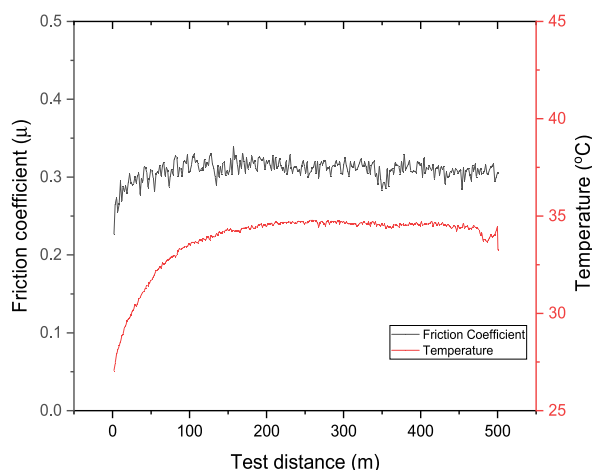
Fig. 6. Friction Coefficient andTemperatureProfile of Pure PPRC as a Function of Sliding Distance.

influencing the composite's tribological properties.

4.3. Coefficient of friction of neat PPRC

Fig. 6 depicts the friction coefficient and temperature increase of pure PPRC sheets as functions of sliding distance. The polymer surface demonstrated a friction coefficient through the continuous sliding of a stainless-steel ball over the sample surface. At the start of the test, a sharp increase in both μ and surface temperature was observed, which might be attributed to the rupture of the polymer surface [36]. This sudden rise in μ led to a temperature increase, reaching approximately 32 °C, with a thin layer of polymer beginning to form on the sliding path.

Once the sliding distance reached 100 m, the surface temperature remained nearly constant, only increasing to about 34 °C after an additional 400 m of sliding distance. Similarly, the friction coefficient showed an almost consistent value. The fluctuations in μ values can be attributed to the rupture of the polymer's top surface and the exposure of a new layer. Moreover, it's plausible that when the sliding distance hit 100 m, the film formation process at the interface achieved a steady state, resulting in an average friction coefficient of 0.30821. A thermal equilibrium was also noticed, possibly due to heat dissipation during film deformation. To further elucidate the tribological behavior of the biocomposite, tests were conducted on all samples under the same conditions.

4.4. Coefficient of friction of WPCs

In the present study, the coefficient of friction (CoF) of WPC samples with varying compositions of rice husk (RH) was investigated. The experimental results suggested that the inclusion of untreated and treated RH in the PPRC polymer matrix markedly affected frictional behavior. Fig. 7 displays the CoF and temperature profiles of the biocomposite samples made from untreated and treated RH, as detailed in Table 1. It's clear that the addition of fillers significantly altered the CoF of PPRC.

Fig. 7a and b represent the 20RH and 20RHT biocomposite samples, respectively. For the 20RH sample, surface friction initially rises sharply during testing before showing slight fluctuations over approximately 200 m of sliding distance. Simultaneously, the specimen's surface temperature also climbs and eventually stabilizes. As the SS ball glides over the specimen, the surface layer starts to rupture, revealing RH particles to the sliding SS ball, thereby further raising the CoF [8]. This results in a fluctuating CoF curve. Microscopic images of the worn specimen surfaces (Fig. 8a) uncover pull-out fibers and debris patches along the tribo-test path. As the sliding distance increases, so does the WPC sheet's temperature, leading to alterations in the CoF profile and the samples' average CoF.

The temperature trend is more pronounced for the 20RHT composite specimen, as illustrated in Fig. 7b. Here, the temperature rises steadily, reaching a peak (Tmax) of 42.5 °C, softening the matrix surface and revealing short RHT fibers. Treated RH, with its high cellulosic fiber content, causes fluctuations in the CoF. Even though the mean CoF values for the 20RH and 20RHT samples are similar, their average values differ substantially due to these fluctuations, recording at 0.2977 and 0.34773, respectively. Fig. 8b presents a micrograph of the irregular surface, debris patches, and intersecting fibers observed on the specimen's sliding path, contributing to its fluctuating behavior.

Regarding the 27.5 % biowaste loading, Fig. 7c and d showcase the CoF of the 27RH and 27RHT samples, respectively. Both charts vividly illustrate how the CoF values demonstrate great variation and considerable standard deviations. This might be due to high fiber loading or inconsistent fiber orientations within the composite matrix.

For the 27RH sample, a 15 °C increase in surface temperature is noted across the test's sliding distance (from $T_0 = 29$ °C to Tmax = 44 °C), which softens the composite's surface, leading to contact between the RH fibers and the SS testing ball. This results in significant CoF fluctuations [8]. The PPRC material's rough texture arises from fiber agglomeration. Additionally, elevated temperatures cause the thin wear layer formed during the tribological cycle to shed, revealing newer material surfaces with a denser fiber content.
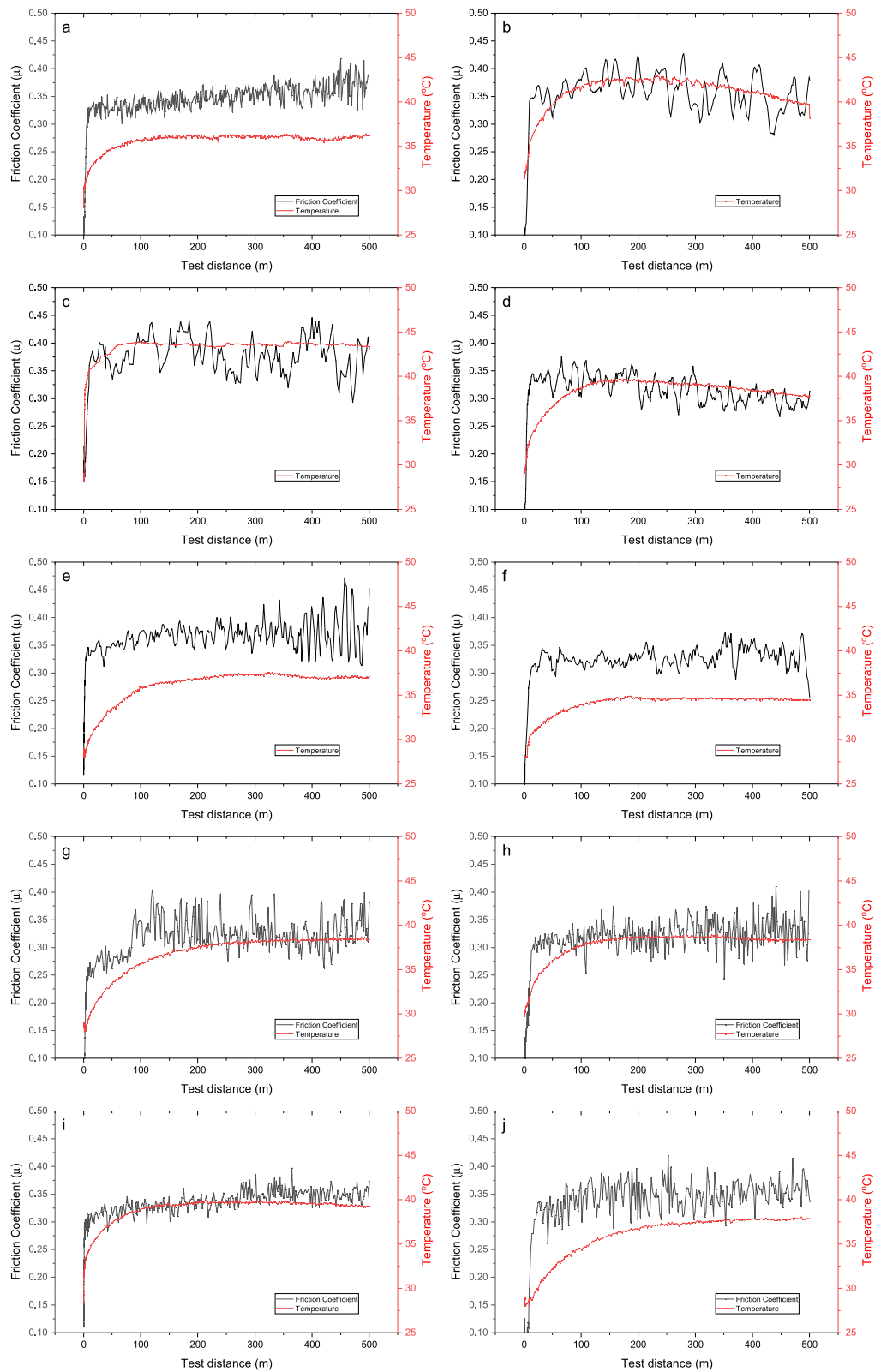
Fig. 7. CoF andTemperature Profiles of WPC Samples as aFunction of Sliding Distance.
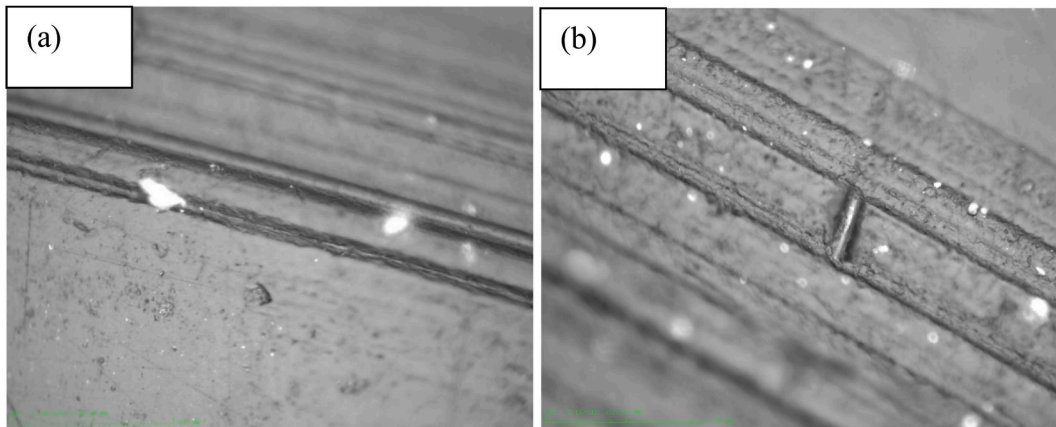
Fig. 8. Microscopic Image of Tribological Path for WPC Synthesized by (a) RH, (b) RHT
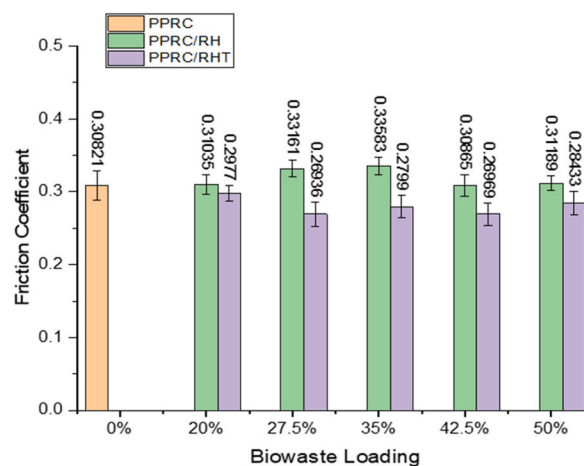

Fig. 9. Mean Friction Coefficient Behavior of PPRC, and WPC Samples for Different Biowaste Loading.

Fig. 7d portrays the frictional traits of the 27RHT specimen. Initially, as the sliding distance reaches about 150 m, the CoF starts climbing until it peaks at 0.36. Concurrently, the surface temperature shows an increase of 11 °C (from $T_o = 28$ °C to Tmax = 39 °C). This scenario hastens the top surface's fracture of the WPC, causing RHT particles to modify the CoF. Beyond a sliding distance of 150 m, the CoF pattern repeats, while the surface temperature dips slightly by 1 °C (from $T_o = 39$ °C to Tmax = 38 °C). This drop may be due to enhanced heat dissipation from fluctuations in the CoF.

For the 35 % biowaste loading, Fig. 7e and f depict the CoF and temperature profiles as a function of sliding distance for the untreated and treated RH in WPC, respectively. According to the results, the 35RH specimen displays a progressive increase in both temperature and CoF up to approximately 100 m. Beyond this point, the rise in temperature stabilizes across the remaining sliding distance. As the sliding ball impacts and extracts RH fibers from the surface, the CoF exhibits a pronounced fluctuation. The heightened filler loading augments the likelihood of fiber interaction with the sliding ball. The untreated material has an average CoF of 0.36637, surpassing that of pure PPRC.

For the 42.5 % biowaste loading, the friction coefficient for both untreated and treated RH is presented in Fig. 7g and h, respectively. Both graphs demonstrate analogous trends. The CoF value escalates for a brief sliding span of around 80 m, but then the 42RH specimen exhibits a sudden surge, inducing pronounced oscillations in the readings. Conversely, the 42RHT specimen maintains a consistent trend without abrupt changes. This distinction might stem from the extraction of fibers from the 42RH specimen, generating significant fluctuations and irregularities on its surface. The temperature patterns for both samples align closely, suggesting that at high filler loadings, the CoF is largely independent of temperature.

Lastly, Fig. 7i and j presents the CoF for the untreated and treated RH at a 50 % loading. The 50RH specimen undergoes a swift temperature ascent of 10 °C within the initial 100 m of sliding, after which it remains relatively stable. The CoF retains a consistent trend throughout the test, implying that the dense fiber content in the WPC sample supports the load, resulting in minimal variations on the surface. In contrast, the 50RHT specimen witnesses a gradual temperature increase, with an 8 °C shift observed around the 250 m mark, followed by a mild rise for the test's duration. The biowaste's treatment affects the WPC surface, manifesting in the sporadic

Table 2
Wear weight loss of WPC Samples.

Sample	20RH	27RH	35RH	42RH	50RH
Wear weight loss (%)	0.001	0.001	0.002	0.001	0.001
Sample	20RHT	27RHT	35RHT	42RHT	50RHT
Wear weight loss (%)	0.001	0.001	0	0	

and fluctuating CoF values throughout the test.

4.5. Comparison of mean friction coefficient

Fig. 9 presents the mean friction coefficient (μ) values with standard deviation for PPRC and WPC samples containing different loadings of RH and RHT. The graph shows that friction coefficient values increase with untreated biowaste but decrease with treated biowaste. In its untreated form, rice husk functions as a friction modifier for PPRC. For the 20RH sample, the friction coefficient registers a minor increment, about 0.69 %, compared to pure PPRC. However, for the 27RH and 35RH samples, μ increases by 7.6 % and 9 %, respectively. This underlines that the introduction of RH modifies the frictional characteristics of pure PPRC.

The friction coefficient values ascend with an increasing concentration of RH, though only by a negligible 0.14 % and 1.1 % for the 42RH and 50RH samples, respectively. This observation concludes that a 35 % RH loading induces the peak friction coefficient in WPC. The friction coefficient values tend to fluctuate when the RH content is augmented beyond this point. Similar tendencies have been documented by Y. Shi et al. [37] regarding μ when amplifying the filler content of PTFE composites filled with $K_2Ti_4O_9$ whisker and $K_2Ti_6O_{13}$. Gehlen et al. [38] conducted analogous studies, introducing 0 %, 6 %, and 12 % concentrations of rice husk into brake friction materials. They discerned an erratic μ at elevated rice husk concentrations, a phenomenon possibly linked to the temperature sensitivity when integrating high volumes of rice husk into polymers, culminating in inconsistent friction coefficient values.

Regarding compositions of treated rice husk (RHT), all specimens reflect a decrement in the friction coefficient compared to PPRC. The 20RHT sample showcases a 3.47 % decline, hinting at a subtle reduction in friction. As the RHT loading swells to 27.5 %, 35 %, 42.5 %, and 50 %, the friction coefficient decrement becomes more pronounced, with reductions of 12.60 %, 9.21 %, 12.48 %, and 7.70 %, respectively. These findings intimate that integrating treated rice husk modifies friction, diminishing the friction coefficient of the WPC samples with respect to PPRC.

The data underscores the ability of treated rice husk to serve as an effective solid lubricant in WPC, leading to improved frictional behavior. However, the reduction in the friction coefficient isn't consistent across different loading concentrations, showing a range of decrease percentages. This variability might arise from the unique composition and behavior of treated rice husk at different concentrations. Similarly, Chin C. et al. [39] found that when PTFE is added to epoxy composites, it acts as a solid lubricant, reducing the friction coefficient compared to pure epoxy. In a related study, Mysiukiewicz et al. [27] explored the effects of oil-rich waste fillers on poly-lactic acid composites. Their findings align with this study, suggesting that fillers act as internal lubricants in PLA composites, with the frictional response changing depending on the filler composition.

4.6. Wear characterization

Wear weight loss is determined by weighing the samples before and after a tribology test over a sliding distance of 500 m. Table 2 presents the wear weight loss percentages for various WPC samples with different compositions in comparison to the PPRC sample. The wear weight loss of the PPRC sample is recorded as 0 %, suggesting no significant wear during the test. This can be attributed to strong intermolecular interactions in pure PPRC.

For WPC samples with untreated rice husk (RH), the wear weight loss percentages vary between 0.001 % and 0.002 %. This indicates that adding RH in different concentrations has minimal influence on the wear resistance of the WPC material. For the WPC samples with treated rice husk (RHT), the wear weight loss percentages range from 0 % to 0.001 %. It suggests that treated rice husk can even enhance the wear resistance of the WPC material compared to the PPRC sample.

WPC samples, irrespective of the rice husk type (RH or RHT), exhibit excellent wear resistance. This indicates that rice husk filler, whether untreated or treated, doesn't compromise the wear performance of the WPC material. The data suggests that wear loss in WPC isn't solely determined by rice husk composition but also by factors like surface temperature.

During tribological testing, two primary surface mechanisms come into play as the temperature rises. The initial abrasion between the polymer and disc generates heat, causing the material to melt and leading to surface fractures and debris. However, a secondary mechanism, adhesion, becomes prevalent with higher biowaste compositions, as the material hardens and exhibits a lower friction coefficient. This causes debris to stick to the WPC surface, potentially reducing wear loss.

In conclusion, several factors play a role in determining wear loss, including the inherent properties of the material, the temperature experienced during testing, and the strength of the binding forces within the composite. As biowaste composition rises, there's a general trend where wear loss also increases, which can be attributed to heightened friction and the subsequent rise in temperature. Intriguingly, when the rice husk concentration reaches 42 % and 50 %, the expected trend is defied due to an unforeseen adhesion mechanism. In these instances, the wear debris adheres back to the WPC surface, which effectively mitigates the wear loss. This counterintuitive behavior underscores the complexity of wear dynamics in composite materials, a phenomenon also noted in studies such as the one by Omrani et al. [40].
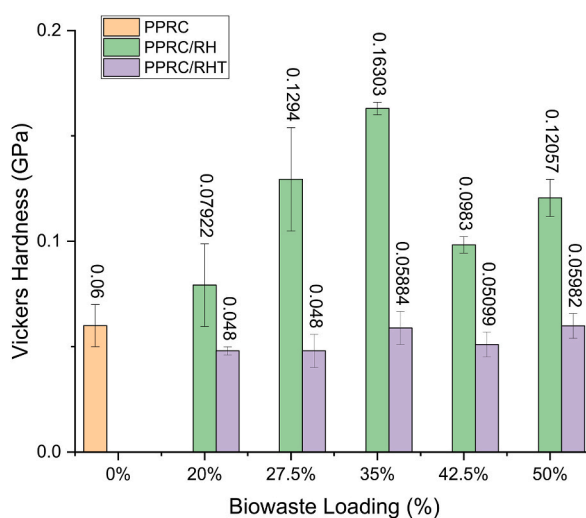
Fig. 10. Vickers Microhardness of PPRC, and WPCSamples for Different Biowaste Loading.

4.7. Vickers Microhardness

Fig. 10 represents the Vickers hardness of pure PPRC and WPC specimens. The Vickers hardness of PPRC samples is measured to be 0.06 ± 0.01 GPa. In contrast, WPC derived from RH and RHT exhibits higher and lower Vickers hardness values than PPRC, respectively. The 20RH sample shows a pronounced increase in hardness, approximately 32 % higher than that of PPRC, suggesting that the integration of rice husk enhances the WPC material's rigidity. As the rice husk loading rises to 27RH and 35RH, the Vickers hardness sees notable augmentations of around 116 % and 172 %, respectively. These findings imply that a greater concentration of rice husk bolsters the hardness properties of the WPC, potentially due to enhanced rigidity, increased resistance to deformation, and cohesive bonding of rice husk fibers with the PPRC, as depicted in FESEM Fig. 3a. Previous studies [41,42] have elucidated that the synergy between fibers and polymers is instrumental in amplifying the resilience of biocomposites, leading to elevated hardness values.

However, upon reaching the 42RH sample with a rice husk loading of 42 %, a marginal decline in Vickers hardness is observed compared to prior samples, though it remains superior to that of PPRC. Likewise, the 50RH sample, which has a 50 % rice husk loading, possesses a Vickers hardness approximately 100 %, slightly beneath the hardness achieved with a 35 % rice husk loading. This reduction might arise from aspects such as the dispersion and orientation of rice husk particles within the composite, which can dictate the composite's overall hardness dynamics. Agglomeration of RH fibers within biocomposites hampers the effective fiber-polymer interaction, culminating in weakened biocomposite sheets [43]. Consequently, Vickers hardness values diminish with escalating biowaste loading. Numerous scholarly articles have documented an upswing in Vickers hardness of polymers up to an optimal content (171 % for 35 % biowaste loading) [44,45], indicating that the peak loading of untreated rice husk for optimal hardness might reside around the 35 % mark.

Transitioning to the samples constructed from treated rice husk (RHT), it's observed that their Vickers hardness values trail those of PPRC. Two elements are pivotal to this downward trend. The first pertains to fiber breakage and inconsistent polymer compatibility, as evidenced in FESEM Fig. 3b and d of treated biocomposite sheets. Additionally, treated rice husk filler is rich in cellulose, which undermines the composite's strength, culminating in a diminished hardness value.

5. Conclusions

In conclusion, the FTIR analysis highlighted the successful integration of rice husk (RH) into the polypropylene random copolymer (PPRC) matrix, with the emergence of distinct peaks underscoring the influence of grafted maleic anhydride and the RH's cellulosic component. The FESEM imagery illustrated a marked difference between untreated and alkali-treated rice husk in WPC samples. While untreated samples showed weaker adhesion at the interface, treated samples exhibited enhanced interlocking, although with some unevenness possibly due to shorter fiber lengths and aggregation. The frictional analyses revealed that untreated RH marginally increased the coefficient of friction at low concentrations and led to erratic behavior at higher concentrations. In contrast, treated RH consistently lowered the coefficient, highlighting its potential as a lubricant for WPCs. Wear characterization further reinforced the WPCs' robustness, with all samples showing minimal wear weight loss. Vickers Microhardness results indicated that RH-enhanced WPCs surpassed the hardness of pure PPRC, with an optimal hardness observed at 35 % RH loading. However, there was a decline in hardness at higher concentrations, while samples embedded with treated rice husk (RHT) exhibited inferior hardness, likely due to fiber damage and high cellulose content. The findings collectively underline the potential of both untreated and treated rice husks in modifying the physical and mechanical properties of WPCs.

Data availability statement

The authors take full responsibility that the data presented in this manuscript has not been published or shared to any other online source/research related article. And there is no conflict of interest among authors.

CRediT authorship contribution statement

Fahad Ali Rabbani: Conceptualization, Investigation, Methodology, Writing – original draft. **Muhammad Sulaiman:** Writing – review & editing, Data curation, Writing – review & editing. **Fatima Tabasum:** Writing – review & editing, Data curation, Formal analysis. **Saima Yasin:** Supervision, Writing – review & editing. **Tanveer Iqbal:** Supervision, Writing – review & editing. **M.A. Mujtaba:** Formal analysis, Software, Writing – review & editing, Formal analysis, Software, Writing – review & editing. **C Ahamed Saleel:** Formal analysis, Software, Writing – review & editing, Formal analysis, Software, Writing – review & editing. **Shahid Bashir:** Funding acquisition, Writing – review & editing. **H. Fayaz:** Funding acquisition, Writing – review & editing.

Declaration of competing interest

The authors declare that they have no known competing financial interests or personal relationships that could have appeared to influence the work reported in this paper.

Acknowledgement

References

[1] S. Kumar, K.K.S. Mer, B. Gangil, V.K. Patel, Synergy of rice-husk filler on physico-mechanical and tribological properties of hybrid Bauhinia-vahlii/sisal fiber reinforced epoxy composites, J. Mater. Res. Technol. 8 (2) (Apr. 2019) 2070–2082, https://doi.org/10.1016/j.jmrt.2018.12.021.

[2] V. Pranay, & S. Ojha, & G. Raghavendra, & G. Dheeraj, and & A. Anjali, "Evaluation of Mechanical and Tribological Properties of Biowaste and Biowaste Based Silica Particulate Epoxy Composites," doi: 10.1007/s12633-021-01227-9/Published.

[3] A.S. Jose, A. Athijayamani, S.P. Jani, A review on the mechanical properties of bio waste particulate reinforced polymer composites, Mater. Today Proc. 37 (Part 2) (2020) 1757–1760, https://doi.org/10.1016/j.matpr.2020.07.360.

[4] T. Francis, N. Dieunedort, D.N. Augustine, G.K.B. Morino, T. Ghislain, N. Ebenezer, Identification of optimal particle size and weight ratio starting from a multi-level statistic analysis concerning tribological performance of Canarium Schweinfurthii shells (CSS)/unsaturated polyester resin (UPR) composites, Tribol. Int. 174 (May) (2022), 107698, https://doi.org/10.1016/j.triboint.2022.107698.

[5] F. Bledzki, Sperber, "natural and wood fibre reinforcement in polymers,", Macromolecules 13 (8) (2002) 3–144.

[6] N. Tripathi, C.D. Hills, R.S. Singh, C.J. Atkinson, Biomass waste utilisation in low-carbon products: harnessing a major potential resource, npj Clim. Atmos. Sci. 2 (1) (2019), https://doi.org/10.1038/s41612-019-0093-5.

[7] R. Liang Dr, G. Hota, Fiber-reinforced polymer (FRP) composites in environmental engineering applications, in: Developments in Fiber-Reinforced Polymer (FRP) Composites for Civil Engineering, Elsevier Inc., 2013, pp. 410–468.

[8] G. Singh, N. Sharma, D. Kumar, H. Hegab, Design , development and tribological characterization of Ti – 6Al – 4V/hydroxyapatite composite for bio-implant applications, Mater. Chem. Phys. 243 (October 2019) (2020), 122662, https://doi.org/10.1016/j.matchemphys.2020.122662.

[9] J. Xu, Y. Kong, B. Du, X. Wang, J. Zhou, Exploration of mechanisms of lignin extraction by different methods, Environ. Prog. Sustain. Energy 41 (3) (May 2022), e13785, https://doi.org/10.1002/EP.13785.

[10] L. Lancaster, M.H. Lung, D. Sujan, A.C.S. Ash, Utilization of agro-industrial waste in metal matrix composites: towards sustainability, Int. J. Environ. Ecol. Eng. 7 (1) (2013) 35–43.

[11] B. Rob, E. Wolter, L. Peter, D. Sietske Boschma, I. Kees, W. Kwant, Rice Straw and Wheat Straw. Potential Feedstocks for the Biobased Economy, Jun. 2013. Accessed: Dec. 26, 2021. [Online]. Available: https://english.rvo.nl/sites/default/files/2013/12/Straw. report AgNL June 2013.pdf.

[12] O. Faruk, M.S. Ain, Biofiber reinforced polymer composites for structural applications, in: N. Uddin (Ed.), Developments in Fiber-Reinforced Polymer (FRP) Composites for Civil Engineering, Woodhead Publishing Limited, 2013, pp. 18–53.

[13] S. Adiloğlu, et al., Use of agro-industrial wastes in solid-state fermentation processes, Industrial Waste i (tourism, Portugal) (2012) 13.

[14] R. Paul, K. Gouda, S. Bhowmik, Effect of different constraint on tribological behaviour of natural fibre/filler reinforced polymeric composites: a review, Silicon 13 (8) (2021) 2785–2807, https://doi.org/10.1007/s12633-020-00613-z.

[15] S. L. S Panthapulakkal, M Sain, "Effect of Coupling Agents on Rice-husk-filled HDPE Extruded Profiles." .

[16] S. Panthapulakkal, S. Law, M. Sain, Enhancement of processability of rice husk filled high-density polyethylene composite profiles, J. Thermoplast. Compos. Mater. 18 (5) (2005) 445–458, https://doi.org/10.1177/0892705705054398.

[17] P.P. Das, V. Chaudhary, Tribological and dynamic mechanical analysis of bio-composites: a review, Mater. Today Proc. 25 (Jan. 2020) 729–734, https://doi.org/10.1016/J.MATPR.2019.08.233.

[18] M. Milosevic, P. Valášek, A. Ruggiero, Tribology of natural fibers composite materials: an overview, Lubricants 8 (4) (2020) 1–19, https://doi.org/10.3390/lubricants8040042.

[19] H. Sumithra, B. Sidda Reddy, A review on tribological behaviour of natural reinforced composites, J. Reinf. Plast. Compos. 37 (5) (2018) 349–353, https://doi.org/10.1177/0731684417747742.

[20] S.M. Terekhina, G.V. Malysheva, I.M. Bulanov, T.V. Tarasova, Investigation of tribological properties of polymer composite materials based on bismaleimide binder, Polym. Sci. - Ser. D 4 (2) (2011) 136–137, https://doi.org/10.1134/S1995421211020158.

[21] M. Sulaiman, T. Iqbal, S. Yasin, H. Mahmood, A. Shakeel, Study of nano-mechanical performance of pretreated natural fiber in ldpe composite for packaging applications, Materials 13 (21) (2020) 1–10, https://doi.org/10.3390/ma13214977.

[22] X. Li, B. Bhushan, A review of nanoindentation continuous stiffness measurement technique and its applications, Mater. Charact. 48 (1) (2002) 11–36, https://doi.org/10.1016/S1044-5803(02)00192-4.

[23] A.M. Díez-Pascual, M.A. Gómez-Fatou, F. Ania, A. Flores, Nanoindentation in polymer nanocomposites, Prog. Mater. Sci. 67 (2015) 1–94, https://doi.org/10.1016/j.pmatsci.2014.06.002.

[24] M.Z. Rong, M.Q. Zhang, G. Shi, Q.L. Ji, B. Wetzel, K. Friedrich, Graft polymerization onto inorganic nanoparticles and its effect on tribological performance improvement of polymer composites, Tribol. Int. 36 (9) (2003) 697–707, https://doi.org/10.1016/S0301-679X(03)00029-X.

[25] F.A. Rabbani, S. Yasin, T. Iqbal, U. Farooq, Experimental study of mechanical properties of polypropylene random copolymer and rice-husk-based biocomposite by using nanoindentation, Materials 15 (5) (2022), https://doi.org/10.3390/ma15051956.

[26] B.-L. Choi, J.K. Jung, B. Un Bong, B.H. Choi, Effect of functional fillers on tribological characteristics of acrylonitrile butadiene rubber after high- pressure hydrogen exposures, Polymers 14 (2022) 861, https://doi.org/10.3390/polym14050861.

[27] O. Mysiukiewicz, J. Sulej-Chojnacka, M. Kotkowiak, T. Wiśniewski, A. Piasecki, M. Barczewski, Evaluation of the oil-rich waste fillers' influence on the tribological properties of polylactide-based composites, Materials 15 (3) (2022), https://doi.org/10.3390/ma15031237.

[28] A.F. Ahmed, S. Sivaganesan, Materials Today : proceedings Characterization of material properties of green polymer composite, Mater. Today Proc. (xxxx) (2023), https://doi.org/10.1016/j.matpr.2022.07.213.

[29] M. Hafizuddin, et al., Effect of alkaline treated rice husk on the mechanical and morphological properties of recycled HDPE/RH composite, J. Appl. Sci. Agric. 10 (5) (2015) 138–144 [Online].

[30] J. Fang, L. Zhang, D. Sutton, X. Wang, T. Lin, Needleless melt-electrospinning of polypropylene nanofibres, J. Nanomater. 2012 (2012), https://doi.org/10.1155/2012/382639.

[31] E.R. Sutjipto, K. Li, S. Pongpattanasuegsa, M.M. Nazhad, Effect of recycling on paper properties, TAPPSA J 0 (cycle 1) (2008) 3–9 [Online], http://tappsa.co.za/archive3/Journal_papers/journal_papers.html.

[32] Y. Zhou, J. Hu, B. Dang, J. He, Mechanism of highly improved electrical properties in polypropylene by chemical modification of grafting maleic anhydride, J. Phys. D Appl. Phys. 49 (41) (2016), https://doi.org/10.1088/0022-3727/49/41/415301.

[33] E. Guilbert-García, R. Salgado-Delgado, N.A. Rangel-Vázquez, E. García-Hernández, E. Rubio-Rosas, R. Salgado-Rodríguez, Modification of rice husk to improve the interface in isotactic polypropylene composites, Lat. Am. Appl. Res. 42 (1) (2012) 83–87.

[34] I.Z. Luna, K.C. Dam, A.M.S. Chowdhury, M.A. Gafur, N. Khan, R.A. Khan, Physical and thermal characterization of alkali treated rice husk reinforced polypropylene composites, Adv. Mater. Sci. Eng. (2015) 2015, https://doi.org/10.1155/2015/907327.

[35] H.J. Jung, K.K. Oh, NaOH-catalyzed fractionation of rice husk followed by concomitant production of bioethanol and furfural for improving profitability in biorefinery, Appl. Sci. 11 (16) (2021), https://doi.org/10.3390/app11167508.

[36] A. Molinari, G. Straffelini, B. Tesi, T. Bacci, G. Pradelli, Effects of load and sliding speed on the tribological behaviour of Ti-6A1-4V plasma nitrided at different temperatures, Wear 203 (96) (1997) 447–454, https://doi.org/10.1016/S0043-1648(96)07419-4. –204.

[37] Y.J. Shi, X. Feng, H.Y. Wang, C. Liu, X.H. Lu, Effects of filler crystal structure and shape on the tribological properties of PTFE composites, Tribol. Int. 40 (7) (2007) 1195–1203, https://doi.org/10.1016/j.triboint.2006.12.006.

[38] G.S. Gehlen, P.D. Neis, L.Y. Barros, J.C. Poletto, N.F. Ferreira, S.C. Amico, Tribological performance of eco-friendly friction materials with rice husk, Wear 500–501 (January) (2022), 204374, https://doi.org/10.1016/j.wear.2022.204374.

[39] C.W. Chin, B.F. Yousif, Potential of kenaf fibres as reinforcement for tribological applications, Wear 267 (9–10) (2009) 1550–1557, https://doi.org/10.1016/j.wear.2009.06.002.

[40] E. Omrani, P.L. Menezes, P.K. Rohatgi, State of the art on tribological behavior of polymer matrix composites reinforced with natural fibers in the green materials world, Eng. Sci. Technol. an Int. J. 19 (2) (2016) 717–736, https://doi.org/10.1016/j.jestch.2015.10.007.

[41] R. Ma, et al., Mechanical properties and in vivo study of modified-hydroxyapatite/polyetheretherketone biocomposites, Mater. Sci. Eng. C 73 (2017) 429–439, https://doi.org/10.1016/j.msec.2016.12.076.

[42] W. Jeong, S.E. Shin, H. Choi, Microstructure and mechanical properties of titanium–equine bone biocomposites, Metals 10 (5) (2020) 1–10, https://doi.org/10.3390/met10050581.

[43] K. Rajkumar, et al., Mechanical and water absorption behaviour of palm seed particles based hybrid bio-composites, J. Phys. Conf. Ser. 2027 (1) (2021), https://doi.org/10.1088/1742-6596/2027/1/012006.

[44] M.S. Abu Bakar, P. Cheang, K.A. Khor, Tensile properties and microstructural analysis of spheroidized hydroxyapatite-poly (etheretherketone) biocomposites, Mater. Sci. Eng. A 345 (1–2) (2003) 55–63, https://doi.org/10.1016/S0921-5093(02)00289-7.

[45] R. Karthick, P. Sirisha, M.R. Sankar, Mechanical and tribological properties of PMMA-sea shell based biocomposite for dental application, Procedia Mater. Sci. 6 (Icmpc) (2014) 1989–2000, https://doi.org/10.1016/j.mspro.2014.07.234.